A Parameterization Scheme of Surface Turbulent Momentum and Sensible Heat over the Gobi Underlying Surface

ZHANG Qiang*[1,3] (张 强), HUANG Ronghui[2] (黄荣辉), and TIAN Hui[3] (田 辉)

[1] *Institute of Arid Meteorology, China Meteorological Administration, Lanzhou* 730020,

[2] *Institute of Atmospheric Physics, Chinese Academy of Sciences, Beijing* 100029

[3] *Cold and Arid Regions Environment and Engineering Institute, Chinese Academy of Sciences, Lanzhou* 730000

(Received March 3, 2002; revised October 21, 2002)

ABSTRACT

The parameterization of surface turbulent fluxes over the Gobi Desert in arid regions is studied by using rationally screened observational data. First, the characteristics of Monin-Obukhov similarity functions are analyzed and their empirical formulae are fitted. The results show that fitted curves of changes of similarity functions of wind speed and temperature with stability parameter differ little from the typical empirical curves and are within the ranges of scatter of the empirical curves, but their values in the neutral condition are different from the typical values to some extent. Furthermore, average values of momentum and scalar (sensible heat) roughness lengths as well as changes of scalar roughness length with friction velocity are determined by utilizing the data. It is found that the average values of scalar roughness length are about one order smaller than that of the momentum roughness length and decrease with increasing friction velocity, but they are evidently larger than their theoretically forecasted values.

Key words: Gobi, surface turbulent flux, parameterization, similarity functions, scalar roughness length

1. Introduction

In most of the present atmospheric numerical models, especially in meso/micro-scale models, the handling of lower boundary physical processes such as surface momentum and sensible heat fluxes is put into a land-surface process model that is coupled with the atmospheric numerical models. In most of the land-surface process models (Monin and Obukhov, 1954), surface momentum and sensible heat fluxes are calculated by using the flux-profile relationship (Carl et al., 1973) based on Monin-Obukhov (M-O) similarity theory (Businger et al., 1971), which can usually be expressed as (Monin and Obukhov, 1954)

$$\frac{\kappa z}{u_*}\frac{\partial V}{\partial z} = \phi_{\rm m}, \tag{1}$$

$$\frac{\kappa z}{\theta_*}\frac{\partial \theta}{\partial z} = \phi_{\rm h}, \tag{2}$$

where κ is the von Karman constant and generally equals 0.4; z the height; u_* the friction velocity, θ_* the characteristic temperature scale; V and θ the mean horizontal wind speed and potential temperature, respectively; and $\phi_{\rm m}$ and $\phi_{\rm h}$ the M-O similarity functions of wind and temperature. In an atmospheric numerical model, formulae (1)–(2) need to be written from their differential forms into their integral forms

$$\frac{V}{u_*} = \frac{1}{\kappa}\left(\ln\frac{z-d}{z_0} - \psi_{\rm m}\right), \tag{3}$$

$$\frac{\theta-\theta_{\rm s}}{\theta_*} = \frac{1}{\kappa}\left(\ln\frac{z-d}{z_{T0}} - \psi_{\rm h}\right), \tag{4}$$

where $\theta_{\rm s}$ is surface potential temperature; $\psi_{\rm m}$ and $\psi_{\rm h}$ are integral forms of $\phi_{\rm m}$ and $\phi_{\rm h}$, respectively; d the displacement height, neglected in the Gobi; z_0 and z_{T0} are the roughness lengths of momentum and sensible heat respectively (the latter is also called scalar roughness length). Concerning the group of equations consisting of formulas (3)–(4), the parameterization of surface turbulent fluxes can be achieved while $\phi_{\rm m}$ and $\phi_{\rm h}$ as well as z_0 and z_{T0} are given.

When M–O similarity theory was established by Monin and Obukhov (1954), the M–O similarity functions were only qualitatively known in theory to be

*E-mail: qzhang@ns.lzb.ac.cn

functions of the M-O atmospheric stability parameter $\zeta(\zeta = z/L$, where the M-O length L can be expressed as $L = (T/\kappa g)/(u_*^2/\theta_*)$, but their thorough forms were not known. The semi-empirical formulae of similarity functions ϕ_m and ϕ_h were first found by Businger et al. (1971) using data of the Kansas experiment. After that, many works (Carl et al., 1973; Bradley et al., 1981; Kai, 1982; Dyer and Hicks, 1970) conducted extensive research on similarity functions. Among many sets of empirical functions fitted by experimental data, there are great differences in the functions' form (Businger et al., 1971; Carl et al., 1973; Kai, 1982). However, popularly accepted forms of the similarity functions are as follows

$$\phi_m = \begin{cases} a_1(1 - b_1\zeta)^{-\frac{1}{4}} & \zeta \le 0 \\ a_1(1 + c_1\zeta) & -\zeta > 0, \end{cases} \tag{5}$$

$$\phi_h = \phi_q = \begin{cases} a_2(1 - b_2\zeta)^{-\frac{1}{2}} & \zeta \le 0 \\ a_2(1 + c_2\zeta) & -\zeta > 0, \end{cases} \tag{6}$$

where all of a_1, b_1, c_1, a_2, b_2, and c_2 are empirical constants. Though most people prefer the set of empirical constants given by Dyer (1974) after synthesizing results of several investigations, differences among the sets of empirical constants, in fact, are rather large. In the sets of empirical constants collected by Sorbjan (1989), a_1 is between 1.0 and 1.06, b_1 between 15.0 and 28.0, c_1 between 9.0 and 16.0, a_2 between 0.74 and 1.2, b_2 between 4.7 and 5.2, and c_2 between 4.7 and 6.2. In general, the differences among sets of empirical formulae of similarity functions, on the one hand, result from complex terrains of observational sites and errors of observational data, and on the other hand, may be related to researchers' methods for processing data.

There have been many works to determine the roughness length of momentum by using observational data. Similarly, in some papers (Zou, 1992; Chen, 1993; Zhang et al., 2002a) the momentum roughness length over the Gobi Desert in Northwestern China has been studied. However, so far there have been few observations and research on the scalar roughness lengths (z_{T0} and z_{q0}). In past atmospheric models or data analyses, the scalar roughness lengths were mostly replaced by the momentum roughness length. Undoubtedly, this gave rise to fairly large errors for calculating surface fluxes. Both Garratt (1992) and Brutsaert (1982) held that the transportation mechanism of momentum is different from that of scalar roughness length and there is a great distinction between the momentum roughness length and the scalar roughness length. Especially over the land surface, the former is generally much larger than the latter.

2. Observational data

The data were observed during the intensive observational period (IOP) from 25 May to 17 June 2000 ("Dunhuang experiment" for short) in Dunhuang in Gansu Province, which is a part of the "Field Observational Experiment on Land-Atmosphere Interaction in Arid Region of Northwestern China" (Zhang et al., 2002b). During the IOP, a micrometeorological composite observational station was installed in the Gobi near Dunhuang oasis, a Portable Atmospheric Mosonet (PAM) station was installed in Dunhuang oasis, and an automatic meteorological station (AMS) was installed in the transition area between the oasis and the desert.

The data, which are analyzed in this paper, were observed in a micrometeorological composite observational station in the Gobi. The station is situated at 40°10'N and 94°31'E with an elevation of 1150 m above sea level, in the Shuangdunzi Gobi to the west of Dunhuang oasis, and the nearest distance of about 7 km to the edge of Dunhuang oasis. Its geographic location and observational site are shown in Fig. 1. Its field is even and pebbly desert. In the Dunhuang region, the mean annual precipitation is about 39 mm and potential annual evaporation comes to 3400 mm. The main wind direction of the observation station is east, and it generally accounts for more than 50% of the observed winds.

At the site, the main observational items include gradients of wind, temperature, and humidity on a tower, radiation components at the surface, temperatures at the surface and in the soil, heat fluxes in the soil, water content and air humidity in the soil, and fluctuations of wind, temperature, and humidity observed by supersonic instruments. The wind, temperature, and humidity on the tower are observed at the four levels of 1, 2, 8, and 18 m high; the sensors of supersonic fluctuation system are 2.9 m high. Surface temperature is indicated by the average of the temperature values observed by using three sensors that are placed at angles 120° from each other and whose observational precision is within 0.02°. Observational precisions of the other instruments are shown in the references (Zhang and Hu, 1992; Wang et al., 1992).

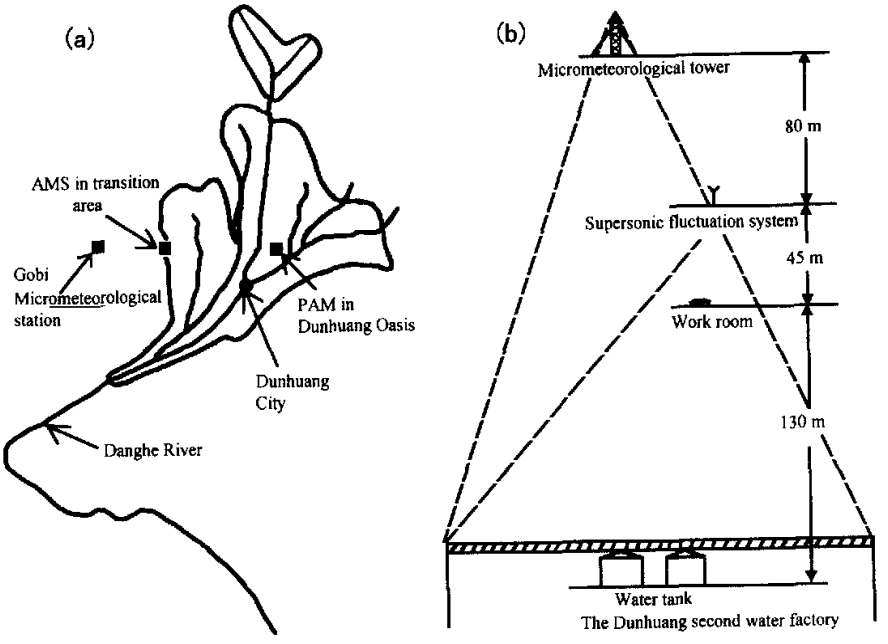

Fig. 1. Geographic location (a) and sketch map of the observational site (b) of Dunhuang Gobi Micrometeorological Central Station.

3. Method of analysis

In order to determine similarity functions ϕ_m and ϕ_h, the differential equations, i.e., formulae (1) (2) need to be transformed into difference equations, and by some mathematical manipulations the following formulae can be obtained

$$\phi_m = \frac{\kappa \Delta V}{u_* \ln(z_{i+1}/z_i)} , \tag{7}$$

$$\phi_h = \frac{\kappa \Delta \theta}{\theta \ln(z_{i+1}/z_i)} , \tag{8}$$

where Δ is the difference symbol and the subscript i denotes vertical stratification. By using the gradient of hourly-averaged wind speed and potential temperature as well as surface turbulent flux, the similarity functions ϕ_m and ϕ_h can be determined.

The momentum roughness length z_0 and scalar roughness lengths z_{T0} and z_{q0} can be calculated by using formulae (3) -(4). After only a little bit of mathematical manipulation, formulae (3)–(4) can be written as

$$z_0 = z \times \exp\left[-\left(\frac{\kappa V}{u_*} + \psi_m\right)\right] , \tag{9}$$

$$z_{T0} = z \times \exp\left\{-\left[\frac{\kappa(\theta - \theta_s)}{\theta_*} + \psi_h\right]\right\} . \tag{10}$$

In the above two formulae, as long as the means of surface temperature, means of wind, temperature, and humidity at any level in the surface layer, and turbulent momentum and sensible heat fluxes are observed, the momentum and scalar roughness lengths can be obtained.

4. Screening of the data

It is the premise of M-O similarity theory that the atmosphere is steady, i.e., possessing temporal stationarity and spatial horizontal homogeneity. Therefore, strictly speaking, to analyze and study parameters related to M-O similarity theory, observation of data must satisfy the conditions that the outside forcing be

basically stationary and the underlying surface basically homogeneous.

First, to avoid weather processes destroying the stationary condition of atmosphere, data observed on cloudy and rainy days are removed. Second, to eliminate the influence of precipitation on changes of soil moisture factor β, those data obviously affected by precipitation (within two days after rainfall) are also canceled. In addition, to eliminate the influence of the unsteady state caused by abrupt changes of solar radiation around sunrise and sunset, those data observed within 3 hours before sunrise and shows after sunset are cut out.

The terrain of the observational site is roughly flat and uniform, but the Dunhuang Second Water Factory is no more than 200 m south of the station (as shown in Fig. 1). Figure 2 shows the histogram of the change of momentum roughness length z_0 and similarity function of wind speed ϕ_m with wind direction. Clearly, when a south wind blows, the momentum roughness length is much larger than in other wind directions, and at most nearly 2 orders larger. Similarly, when a south wind blows, the similarity function of wind speed is strikingly larger than in other wind directions as well. This shows that the Dunhuang Second Water Factory interferes with the dynamical field of the observational station and makes the momentum roughness length in the wind directions affected by it very large. This can cause large errors in the determined similarity functions and roughness lengths.

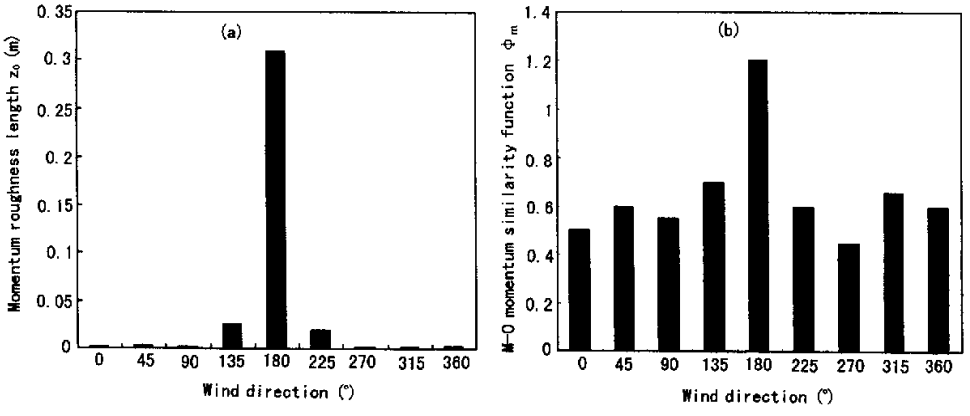

Fig. 2. Histogram of the change of momentum roughness length z_0 (a) and similarity function of wind speed ϕ_m (b) with wind direction.

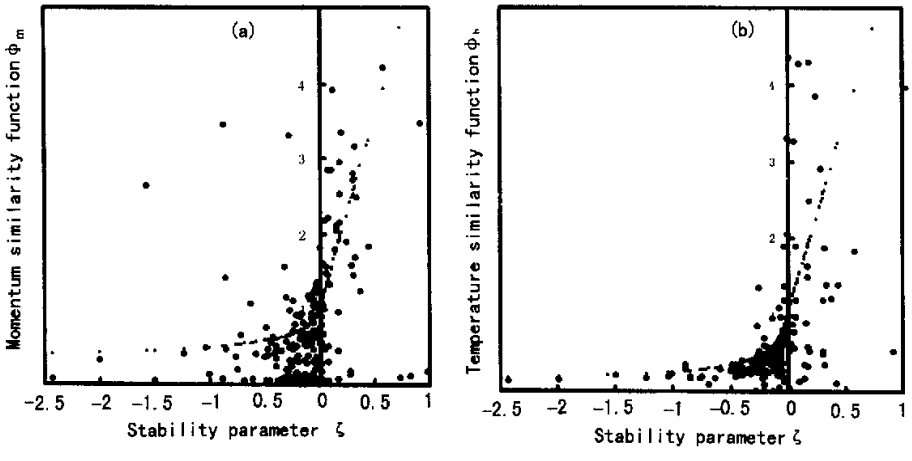

Fig. 3. Variation of M–O similarity function ϕ_m (a) and ϕ_h (b) with M O stability parameter; among the rest, the curves demonstrate empirical relationships given in the reference (Dyer, 1974).

In Fig. 3, the variation of the M–O similarity function ϕ_m and ϕ_h with the M-O atmospheric stability parameter is given. In the figure, the curves present the empirical relationship given in the reference (Dyer, 1974). The figure shows that although the same tendencies of change as the empirical relationships are taken on by fitting the data, the scatter of the data is very large, and sometimes the fitted curves distinctly deviate from the empirical formulae. This mainly reflects the great impact of obstacles near the observational station on fitted formulae of similarity functions. As a consequence, to remove the impacts on the observation of the buildings near the station, those data in the wind direction range from 130° to 190° are cut off.

Meanwhile, in averaging roughness lengths, to avoid the bad effect caused by the imprecision of the empirical formulas of similarity functions ϕ_m and ϕ_h, only those data in which the atmospheric stability parameters calculated from them are between -0.1 and 0.1 are adopted.

5. Analysis of the results

5.1 *Fitting of the M–O similarity functions*

In Fig. 4, the variations of the M-O similarity functions ϕ_m and ϕ_h with M O atmospheric stability parameter are given by using those data without interference of the buildings. By making a comparison between Fig. 4 and Fig. 3, it is shown that after the data interfered by the buildings are cut off, the scatter of the fitted curves clearly becomes small. And from Fig. 4, it is found for either ϕ_m or ϕ_h that the scatter of their fitted curves in unstable atmosphere are smaller than those in stable atmosphere. This is consistent with the results given in previous research. In stable atmosphere, the effectiveness of fitting ϕ_m is better than that of fitting ϕ_h. In the two small figures in the upper left part of Fig. 4a and b, the changes of ϕ_m and ϕ_h with stable parameter near to the neutral state are given; their fitted relationships are as follows,

$$\phi_m = 0.83 + 1.9\zeta \quad , \quad |\zeta| < 0.1 \ , \tag{11}$$

$$\phi_h = 0.73 + 3.0\zeta \quad , \quad |\zeta| < 0.1 \ . \tag{12}$$

It is shown that in the neutral state, values of ϕ_m and ϕ_h are equal to 0.83 and 0.73 respectively and the value of ϕ_m has some difference from the value determined by Businger et al. (1971). However, while the scatter of our fitted curve is evidently larger than that by Businger et al. (1971), it is understandable that there is very little discrepancy between the two results. The value of ϕ_h in the neutral state is rather close to the typical value of 0.74 (Businger et al., 1971). Values 0.83 and 0.73 can serve as a_1 and a_2 in formulae (5) and (6) respectively. From this, curves of ϕ_m and ϕ_h in the whole range of stability parameter ζ can be

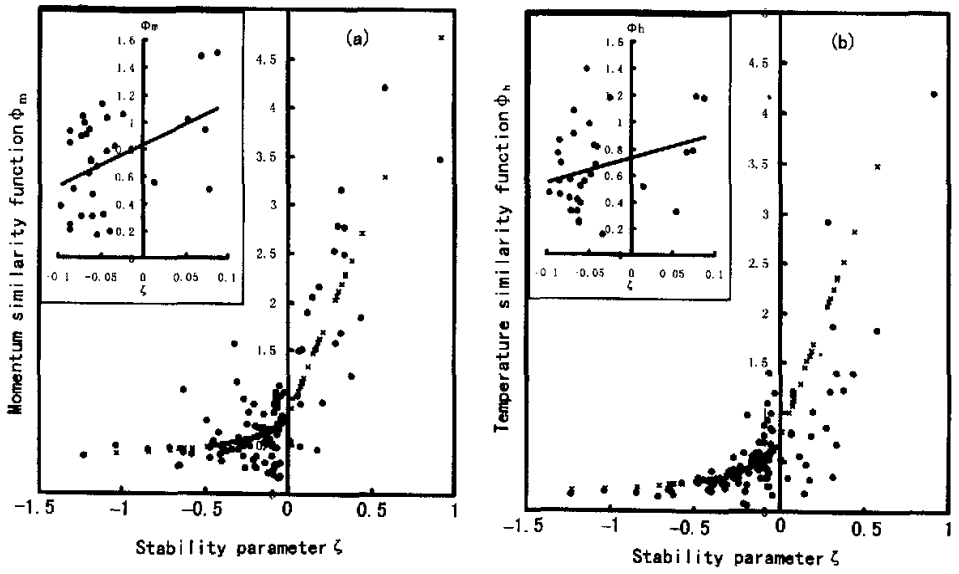

Fig. 4. Variation of M-O similarity function ϕ_m (a) and ϕ_h (b) with M-O stability parameter, the data observed in the "Dunhuang Experiment" and having removed the interference of the buildings, the two small figures are magnified for the neutral state, the solid curves are fitted curves.

fitted as shown in Fig. 4 and the fitted formulae are as follows,

$$\phi_{\rm m} = \begin{cases} 0.83(1-14.6\zeta)^{-\frac{1}{4}} & \zeta \le 0 \\ 0.83(1+4.2\zeta) & \zeta > 0 \ , \end{cases} \tag{13}$$

$$\phi_{\rm h} = \begin{cases} 0.73(1-10.0\zeta)^{-\frac{1}{2}} & \zeta \le 0 \\ 0.73(1+4.8\zeta) & \zeta > 0 \ , \end{cases} \tag{14}$$

where the b_1, b_2, c_1, and c_2 in formulae (5) and (6) are 14.6, 10.0, 4.2, and 4.3, respectively. There are only minor differences between them and the typical values (15, 9, 4.7 and 4.7) and the differences are within the scatter ranges of former empirical values.

5.2 *Characteristics of scalar roughness*

Considering momentum lengths z_0 and scalar roughness lengths z_{T0} in logarithmic form (M-O similarity expressions) in atmospheric models or data analysis, to remove the impact of some extreme points in averaging roughness lengths, a logarithmic average method is adopted as follows

$$\overline{z_0} = \exp(\sum_{i=1}^{n} \ln z_{0i})/n \ , \tag{15}$$

$$\overline{z_{T0}} = \exp(\sum_{i=1}^{n} \ln z_{T0i})/n \ . \tag{16}$$

where the subscript i is a time series. In general, the logarithmically averaged roughness is obviously smaller than the generally averaged ones. It means that the effect of a few extremely large roughness lengths on the mean of roughness length has been partly removed. The logarithmically averaged momentum lengths z_0 and scalar roughness lengths z_{T0} are given in Table 1.

It is thus clear that momentum roughness over the Gobi Desert is a bit smaller than that observed in the Tibetan Plateau regions (Liu et al., 2002), but they are on the same order of magnitude. The mean of momentum roughness length is one order of magnitude larger than that of the scalar roughness length. It has been known by some (Brutsaert, 1922) that on land-surface momentum roughness length is by far larger than scalar roughness length. The reason, which was pointed out by Garratt (1992), is that on the one hand in formula (4), the skin temperature is usually replaced by surface temperature; yet more importantly, momentum transport in the viscous sublayer near the surface mainly depends upon effective drag produced by viscosity shear and the roughness element, but scalar transports such as sensible heat merely rely on the molecular viscous process, therefore, relatively speaking, momentum can be more easily transported than sensible heat. On account of this bottleneck effect, the damping of trangport of momentum in the surface layer is bound to be smaller than that of transporting a scalar quantity such as sensible heat, so a smaller scalar roughness length in formula (4) than that of momentum in formula (5) is required. This means that the Reynolds similarity supposition, which assumes the momentum and scalar transport mechanism is consistent, is no longer tenable (Zhang et al., 2002b).

The momentum roughness length as a parameter of the surface geometry is a local characteristic parameter. According to the above mechanism analysis, scalar roughness length relates not only to the surface geometry but also to turbulent dynamical characteristics of the atmosphere, and is a dynamic parameter. Based on some assumptions, the theoretical relation has been derived by some research (Garratt, 1992) as follows

$$z_{T0} = z_0 7.4 \exp[-7.3\kappa(u_* z_0/v)^{1/4} Pr^{1/2}] \ , \tag{17}$$

where v is the molecular viscosity coefficient; and Pr is the Prandtl number, a parameter to characterize the capability of molecular viscosity and is generally 0.71. It is thus clear that the scalar roughness length theoretically is not only in proportion to momentum roughness length but also closely connected with friction velocity.

In Fig. 5, the changes of observed sensible heat roughness length z_{T0} and its ratio to momentum roughness length z_{T0}/z_0 with friction velocity are given. It shows that sensible heat roughness length z_{T0} remarkably goes down with increasing friction velocity. Thus, the empirical formula is fitted in the form of formula (17) as

$$z_{T0} = 20.5 z_0 \exp[-26.1(z_0 u_*)^{1/4}] \ . \tag{18}$$

When friction velocity is fairly small, sensible heat roughness length z_{T0} can reach the order of millimeters

Table 1. Logarithmically averaged values of momentum and scalar roughness lengths

	Momentum roughness (m)	Sensible heat roughness (m)
Roughness length	0.0019 ± 0.00071	0.00043 ± 0.00032

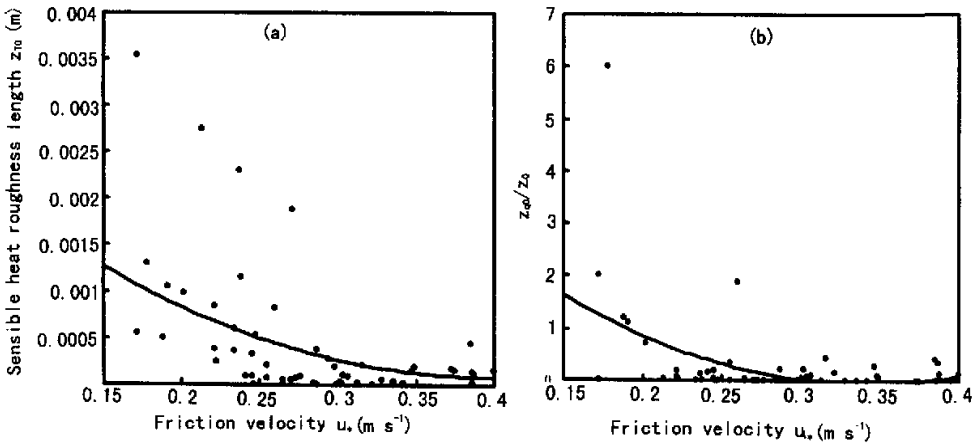

Fig. 5. Change of sensible heat roughness length z_{T0} (a) and its ratio to momentum roughness length z_{T0}/z_0 (b) with friction velocity.

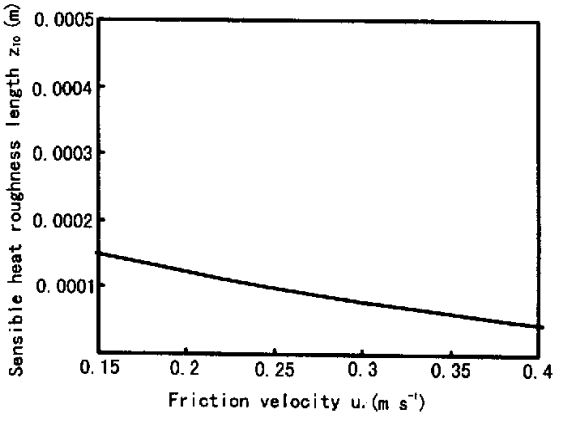

Fig. 6. Theoretical curves of variations of scalar roughness lengths z_{T0} with friction velocity (z_0=0.001 9 m) in formula (17).

and is commensurate with momentum roughness length. But in more cases, the sensible roughness length is only on the order of 10^{-4} m or even smaller, and one order smaller than momentum roughness length.

In Fig. 6, the theoretical curve of variations of scalar roughness lengths z_{T0} with friction velocity (given that momentum roughness length is 0.001 9 m) as given according to formula (17). Clearly, though the theoretical curve roughly shows the same tendency as the observational one, the theoretical values are evidently smaller than the observed ones, especially when friction velocity is rather small, the theoretical values are nearly one order smaller than the observed ones. This means that the theoretical expressions based on some assumptions actually underestimate the value of the scalar roughness lengths.

6. Conclusion and discussion

By utilizing the data observed in "the Dunhuang experiment", better fitted formulas of M-O similarity functions ϕ_m and ϕ_h are obtained, and there is only a little difference between the set of formulae introduced here and the typical ones. What is more, most of the empirical constants in the formulae are basically within the scatter range of the former empirical values, but the value of ϕ_m in the neutral state is a bit smaller.

The logarithmically averaged values of momentum length z_0 and scalar roughness length z_{T0} are 0.001 9, and 0.000 43, respectively; the scalar roughness lengths (z_{T0}) are one order smaller than momentum roughness

lengths z_0, but they are both larger than the theoretically forecasted values.

Scalar roughness length z_{T0} is in proportion to momentum roughness length z_0 and also relies on the nature of atmospheric turbulent dynamics. The observed data shows that scalar roughness length decreases strikingly with increasing friction velocity and approaches the theoretical formula, but is evidently smaller than the theoretical value when friction velocity becomes very small.

The interference of the nearby buildings during the determination of momentum and scalar roughness lengths as well as the M-O similarity functions is very strong, so it is necessary to make a proper screening of observed data in any analysis and research, yet it is also just a premise that this research can be achieved successfully to some extent.

Besides, in arid regions, the study of the water vapor transport mechanism and distribution of specific humidity requires higher precision, so great effort in the observational experiment is necessary for further studies.

Acknowledgments. Theauthors wouldlike to thank Wei Guoan, Hou Xuhong, HouPing and Nie Yanjiang for their help. This work was supported by the National Natural Science Foundation of China under Grant No. 40175004 and the National Key Program for Developing Basic Sciences of China under Grant No. G1998040904 2.

REFERENCES

Bradley, E. F., R. A. Antonia, and A. J. Chambers, 1981: Temperature structure in the atmospheric surface layer, Part 1 and Part 2. *Bound. Layer Meteor.*, **20**, 275 307.

Businger, J. A., J. C. Wyngaard, Y. Izumi, and E. F. Bradley, 1971: Flux profile relationships in the atmospheric surface layer. *J. Atmos. Sci.*, **28**, 181–189.

Brutsaert, W., 1982: *Evaporation into the Atmosphere*, D. Reidel Publishing Company, Dordrecht, Holland, 299pp.

Carl, D. M., T. C. Tarbell, and H. A. Panofsky, 1973: Profiles of wind and temperature from towers over homogeneous terrain. *J. Atmos. Sci.*, **30**, 788–794.

Chen J. Y., Wang J. M., and H. Mitsuaki, 1993: An independent method to determine the surface roughness length. *Chinese J. Atmos. Sci.*, **17**(1), 21–26. (in Chinese)

Dyer, A. J., and B. B. Hicks, 1970: Flux gradient transport of heat and water in an unstable atmosphere. *Quart. J. Roy. Meteor. Soc.*, **93**, 501 -508.

Dyer, A. J., 1974: A review of flux-profile relations. *Bound.-Layer Meteor.*, **7**, 363–372.

Garratt, J. R., 1992, *The Atmospheric Boundary Layer*, Cambridge University Press, Combridge, 89–93.

Kai, K. 1982: Statistical characteristics of turbulence and the budget of turbulent energy in the surface boundary layer. Environmental Research Center Paper No.1, University of Tsukuba.

Liu H. Z., Zhang H. S., Bian L. G., and Chen J. Y., 2002: Characteristics of micrometeorology in the surface layer in the Tibetan Plateau. *Advances in Atmospheric Sciences*, **19**(1), 73–88.

Monin, A. S., and A. M. Obukhov, 1954: Basic laws of turbulent mixing in the atmosphere near the ground. *Tr. Geofiz. Inst. Akad. Nauk SSSR*, **24**(151), 163–187.

Sorbjan, Z. 1989: *Structure of the Atmospheric Boundary Layer.*, Prentice-Hall Inc., 317pp.

Wang J. M., Cui T. M., Y. Mitsuta, and H. Mitsuaki, 1992: A real-time, low cost turbulence data acquisition and processing system. *Plateau Meteor.*, **11**(4), 451–490. (in Chinese)

Zhang Q., and Hu Y. Q., 1992: The instrumental accuracy and observational error about micrometeorological mast of Chinese side in "HEIFE". *Plateau Meteor.*, **11**(4), 460–469. (in Chinese)

Zhang Q., Cao X. Y., Wei G. A., and Huang R. H., 2002a: Observation and study on land surface parameters over Gobi in typical arid region. *Advances in Atmospheric Sciences*, **19**(1), 121–135.

Zhang Q., Wei G. A., and Huang R. H., 2002b: The study of the atmospheric bulk transfer coefficient over Desert and Gobi in arid region of northwestern China. *Science in China (Series D)*, **45**(5), 468 480.

Zuo H. C., Hu Y. Q., 1992: The bulk transfer coefficient over Desert and Gobi in the Heihe region. *Plateau Meteor.*, **11**(4), 371–380. (in Chinese)

荒漠戈壁下垫面表面动量和感热湍流通量参数化研究

张 强 黄荣辉 田 辉

摘 要

用合理筛选以后的野外观测资料，研究了荒漠戈壁地表湍流通量参数化的问题。首先，分析了Monin-Obukhov相似函数的特征，并拟合出了其经验公式。结果表明，风速和温度相似性函数随稳定度参数的变化曲线与典型经验曲线差异较小，并且在经验曲线分布范围以内，但中性时的值有所不同。同时，还用该资料给出了动量和标量粗糙度（感热粗糙度）长度的平均值及其标量粗糙度随摩擦速度的变化关系。发现标量粗糙度的平均值大约比动量粗糙度的小一个量级，并且随摩擦速度的增大而减小，但明显比其理论预测值要大。

关键词： 戈壁，地表通量，参数化，相似性函数，标量粗糙度